

INELASTIC BEHAVIOR OF BUILDING SYSTEMS SUBJECTED TO THREE-DIMENSIONAL EARTHQUAKE MOTIONS

by
Franklin Y. Cheng^I and Prasert Kitipitayangkul^{II}

I. SYNOPSIS

An analytical study is presented for investigating the effect of interacting three dimensional ground motions on the response behavior of elastic and inelastic building systems consisting of steel and concrete members. The earthquake inputs can be applied in any direction of the structural plan for which the P- Δ effect of the second-order moment resulting from the gravity load and the vertical ground motion is considered. Numerical results show that interacting horizontal components can significantly increase the internal forces and the lateral displacements of a structure and thus cause remarkable permanent deformations. The amount of the influence depends on the geometric condition of the structural plan and elevation. A vertical ground motion decidedly increases axial forces but only slightly increases the moments of columns.

II. INTRODUCTION

As an extension of Cheng's previous work of studying the effect of the interacting one horizontal and a vertical ground motion on the response behavior of inelastic plane structures, recent studies were emphasized on the effect of multicomponent earthquakes on the response behavior of elastic and inelastic three-dimensional structures. This paper abstracts some research results from a recent report¹ and deals with only the building systems. The studies of space frames can be found elsewhere.² The detailed mathematical formulation and the extensive references must be referred to Ref. 1.

The structural model is developed for typical building constructions. The characteristics of and the general considerations for the model are as follows: (1) The structure consists of steel columns, beams, and bracings as well as of concrete floor diaphragms, shear walls, and flexural shear panels. The floor plan does not need to be rectangular to which the horizontal ground motions can be applied in any direction. However, the floor levels must be horizontal, and the columns, shear walls, and panels must be vertical. (2) The floor and roof diaphragms are idealized as laminae having infinite rigidity in their own planes but flexibility out of them. Because of the rigidity, each floor can have three common degrees of freedom: two translations and one rotation. However, the individual columns can have axial and torsional deformations and be able to bend about strong and weak axes. The finite length of the rigid structural joint is considered. (3) The structure can be subjected to static vertical loads on beams and joints and lateral loads at the floor levels as well as to three-dimensional interacting ground motions. The mass at each floor produces two transverse and one rotational inertial force and vertical inertial forces at

^IProfessor of Civil Engineering; ^{II}Post-doctoral Fellow, formerly Graduate Research Assistant in Civil Engineering; University of Missouri-Rolla, Rolla, MO 65401, USA.

each column. The dead load of all the floor masses and their inertial forces are included in the analysis as the P-Δ effect. (4) The Ramberg-Osgood hysteresis loops (Fig. 1) are employed to derive the axial, bending, and torsional stiffnesses of the steel members. The Bauschinger effect on the stress reversal is considered during the cycling response. The simplified Takeda model (Fig. 2) is used for reinforced concrete members. The effect of the interacting biaxial bending, axial load, and torsion on the yielding surface is considered for the columns. The shear walls and panels are basically treated as plane elements on which the significant moments are only those that exist about the major axis.

III. METHOD OF ANALYSIS

1. Structural Formulation. Because the lumped masses at each floor are associated with the floor displacements of two translations and one rotation as well as with the axial deformations of the columns, the rotational degrees of freedom at the structural joints can be condensed in the motion equation for the purpose of increasing the computation efficiency. For a typical frame of stories, m and n, the force-displacement relationships can be expressed as

$$\begin{Bmatrix} R_m^f \\ R_n^f \\ R_v^f \\ R_\ell^f \end{Bmatrix} = \begin{bmatrix} K_{mm} & K_{mn} & K_{mv} & K_{m\ell} \\ & K_{nn} & K_{nv} & K_{n\ell} \\ & & K_{vv} & K_{v\ell} \\ \text{Symm} & & & K_{\ell\ell} \end{bmatrix} - \begin{bmatrix} 0 & 0 & 0 & 0 \\ & 0 & 0 & 0 \\ & & 0 & 0 \\ \text{Symm} & & & G_{\ell\ell} \end{bmatrix} \begin{Bmatrix} r_m^f \\ r_n^f \\ r_v^f \\ r_\ell^f \end{Bmatrix} \quad (1)$$

in which the superscript f signifies the reference coordinates of the structural plan of which the direction and the origin can be conveniently chosen, r_m^f and r_n^f denote the joint rotations at floor levels m and n; r_v^f represents the axial displacements of the columns, and r_ℓ^f is associated with the rigid-body motions of the translations and rotations of the structure. It is apparent that the beams at level m contribute stiffness to K_{mm} , K_{mv} , and $K_{v\ell}$; other constituent members contribute to all the other stiffness submatrices. The second-order matrix has only the submatrix, $G_{\ell\ell}$, associated with the lateral floor-displacements. The load vector, R_m^f , represents the fixed-end moments at the joints that result from the static vertical loads, which act on the beams at level m plus the forces from the previous elimination. Similarly R_n^f is for level n. The forces R_v^f and R_ℓ^f not only act in column axial and floor lateral directions respectively, they also include forces resulting from the joint-rotation elimination. After the joint rotations are eliminated for floor, m, then the subscript n becomes m for a new floor below, which will then be represented by n. Thus, after the elimination is completed for the joint rotations at all the story levels except the ground level, one is left with a vertical and lateral stiffness, which is then combined with the second-order matrix to yield the system matrix in the reference coordinates. In order to have a diagonal mass matrix for simplifying the dynamic analysis, the global coordinates of the system must be chosen at the mass centers of the different floors through which earthquake motions are assumed to be acting. Thus, the displacements (two lateral and one rotational) at the mass center of each

story segment and the vertical displacements at the column-ends (not including the ground level) can be considered to be the global coordinates.

2. Solution Technique. Let the incremental dynamic motion equation including the P-Δ effect be expressed in global coordinates as

$$\underline{M}\Delta\ddot{\underline{r}} + \underline{c}\Delta\dot{\underline{r}} + (\underline{K}_e - \underline{K}_g)\Delta\underline{r} = -\underline{M}\Delta\ddot{\underline{r}}_g \quad (2)$$

in which \underline{M} = diagonal mass matrix, \underline{c} = damping matrix, expressed as $\alpha\underline{M} + \beta(\underline{K}_e - \underline{K}_g)$; \underline{K}_e = structural stiffness matrix; \underline{K}_g = geometric stiffness matrix including \underline{M}_g and $\underline{M}^T\underline{r}_g$; $\Delta\underline{r}$, $\Delta\dot{\underline{r}}$, $\Delta\ddot{\underline{r}}$ = incremental displacement, velocity, and acceleration vectors, and $\Delta\ddot{\underline{r}}_g$ = ground acceleration vector including the vertical ($\Delta\ddot{V}_g$) and horizontal ($\Delta\ddot{V}_x$, $\Delta\ddot{V}_y$) components. Based on the step-by-step integration method,³ Eq. 2 can be expressed as

$$\begin{aligned} (1 + \frac{3}{\Delta t}\beta)\underline{K}\Delta\underline{r} + (\frac{6}{\Delta t^2} + \frac{3\alpha}{\Delta t})\underline{M}\Delta\underline{r} - \beta\underline{K}\underline{B}_n - (\frac{6}{\Delta t^2} + \frac{3\alpha}{\Delta t})(\frac{1}{1 + \frac{3}{\Delta t}\beta})\beta\underline{M}\underline{B}_n \\ = \Delta\underline{P} + \underline{M}(\underline{A}_n + \alpha\underline{B}_n) - (\frac{6}{\Delta t^2} + \frac{3\alpha}{\Delta t})(\frac{1}{1 + \frac{3}{\Delta t}\beta})\beta\underline{M}\underline{B}_n \end{aligned} \quad (3)$$

in which Δt is the time interval; n represents the response time; $\underline{A}_n = (6/\Delta t)\dot{\underline{r}}_{n-1} + 3\ddot{\underline{r}}_{n-1}$; $\underline{B}_n = 3\dot{\underline{r}}_{n-1} + (\Delta t/2)\ddot{\underline{r}}_{n-1}$; $\underline{K} = \underline{K}_e - \underline{K}_g$, and $\Delta\underline{P} = -\underline{M}\Delta\ddot{\underline{r}}_g$. Let $c_0 = 3/\Delta t + 6/\Delta t^2$, $c_1 = 1/c_4$, $c_2 = c_0 c_1$, $c_3 = \alpha - c_2 \beta$, $c_4 = 1 + 3\beta/\Delta t$, then Eq. 3 becomes

$$\underline{K} \underline{\bar{r}} = \Delta \underline{\bar{P}} \quad (4)$$

in which $\underline{K} = \underline{K} + c_2 \underline{M}$, $\Delta \underline{\bar{r}} = (1/c_1)\Delta\underline{r} - \beta\underline{B}_n$, and $\Delta \underline{\bar{P}} = \underline{M}(-\Delta\ddot{\underline{r}}_g + \underline{A}_n + c_3 \underline{B}_n)$. The expression of the pseudal dynamic equation in Eq. 4 is identical to the force-displacement relationship for static loads. Thus the well-known Gaussian elimination technique can be used both for static and dynamic cases. In the solution procedures, the displacements at the foundation are set to zero; the complete computation of local displacements and member forces are then carried out floor by floor.

IV. NUMERICAL EXAMPLES

More than one hundred cases of several typical structures were included in Ref. 1 from which two structures with several loading cases are presented herein. The effect of the interaction of the three earthquake components on the response was investigated by considering (c) the N-S component with the P-Δ effect of dead load, (d) the N-S and E-W components with the P-Δ effect of dead load, and (e) the N-S, E-W, and vertical components with the P-Δ effect of both dead load and the vertical earthquakes. Thus the ratio, d/c , indicates how the E-W component affects the response behavior, e/d shows the increase caused by the vertical ground motion, and e/c signifies the influence of both the E-W and vertical components. The structures were analyzed by using the El Centro, 1940 earthquake with a unit scale for which the N-S and E-W components were applied respectively along the N-S and E-W directions of the structural plan. The moduli of elasticity for steel and concrete are 30,000 ksi (20,684 kN/cm²) and 3,000 ksi (2,068 kN/cm²), respectively. The time interval Δt is 0.005 sec.

1. Ten-Story Elastic Reinforced Concrete Building With Symmetric Plan and Shear Panels. The structure is shown in Fig. 3 in which the shear panels

identified as members 9 and 10 are placed at the east and west sides of the building. The maximum ratios, d/c and e/c , of the axial forces of all the columns at each floor are plotted in Fig. 4 in which the curve of e/d signifies the maximum ratios of moments in the E-W plane at the top of columns.

2. Eight-Story Unbraced Steel Building with L-Shape Plan for (A) Undamped and Elastic of $r=1$, (B) Five Percent Damping and $r=20$, (C) Five Percent Damping and $r=80$, and (D) Undamped and $r=20$. The example shown in Fig. 5 represents the analysis of an unsymmetric building for elastic, inelastic, and elasto-plastic cases corresponding to $r=1$, 20, and 80 respectively (see Fig. 1). The five percent damping is expressed in terms of the mass and stiffness as $\alpha=0.4305$ and $\beta=0.00581$. The mass center is at point "A" for which the torsional masses are 62,111.8 k-in-sec² (715,604 kg-m-s²) for the first and second floor, 55,900.62 k-in-sec² (644,044 kg-m-s²) for the third through fifth floor, and 49,689.44 k-in-sec² (572,483 kg-m-s²) for the sixth through eighth floor. The masses associated with the axial displacements of columns are distributed according to the dashed lines shown in the plan and the floor masses shown in the elevation. For the elastic systems (A), the displacements in the x-, y-, and θ (torsional)-direction at the top floor of col. 1 (reference point) are shown in Figs. 6-8 respectively; the vertical displacements shown in Fig. 9 are for col. 4 at the top. For the systems (B) through (D), the comparative studies of the displacements in the x-, y-, rotational and vertical directions are shown in Figs. 10-17 for col. 1 at the top floor; comparisons of the input energy and the dissipated energy are sketched in Figs. 18-20; Figs. 21-23 reveal the comparisons of the maximum ductility factors in the x-direction of the columns for which the ductility is based on the energy absorption.¹ The observations of the results are included in Conclusions.

V. CONCLUSIONS

1. Symmetric Elastic System. The concluding remarks of the effect of the interacting ground motions on (I) internal forces and (II) nodal displacements are derived from the example shown in Fig. 3. (I) A horizontal component acting in one direction can slightly affect the column moments acting in the plane perpendicular to the earthquake motion. However, the interacting horizontal components can induce significant moments in that plane and can significantly increase the axial forces of some columns. The vertical earthquake motion can strongly affect the axial forces but slightly influence the bending moments. (II) The horizontal component, when applied alone in one direction, as in the x-direction, does not induce any noticeable displacement in the y-direction. However, the inclusion of the horizontal component in the y-direction and the vertical component can influence the displacements in both directions. The influence on the displacements in the y-direction is much greater than those in the x-direction.

2. Unsymmetric Elastic and Inelastic Systems. For the example of Fig. 5 the concluding remarks are summarized into four groups as (I) displacement response, (II) energy absorption, (III) ductility factors, and (IV) the influence of plastic models. (I) The horizontal component acting alone in the x-direction can induce the displacements in both the x- and y-directions. The inclusion of an additional horizontal component and the vertical component can cause a considerable amount of permanent deformation in the torsional and y-directions. The increase of the horizontal

displacements is mainly due to the interacting horizontal components but slightly due to the vertical component. The axial displacements of a column are heavily affected by the vertical component but moderately influenced by the horizontal components. (II) The energy absorption characteristics may be numerically expressed in terms of the ratio of the total input energy to the total dissipated energy. The ratios for loading cases (c), (d), and (e) are respectively equal to 1.50, 1.40, and 1.37 for system (B), 1.48, 1.54, and 1.62 for system (C), and 1.50, 1.34, and 1.45 for system (D). The seismic input energies of loading cases (d) and (e), expressed in terms of the input energy of case (c), are respectively equal to 2.00 and 2.11 for system (B), 3.05 and 3.48 for system (C), and 2.24 and 2.22 for system (D). The comparisons apparently show that the interacting ground motions induce more input energy to the structure than the one-dimensional ground motion and then cause more damage to the system. At the end of the earthquake duration, the errors in the energy balance, that is the ratio of the difference between the total input energy and the total output energy to the total input energy, vary from -0.0374 to 0.0119 percent. These small errors indicate that the numerical integrations are extremely accurate. (III) When a structural plane is symmetric, one horizontal component acting alone in the x-direction only demands the ductilities in that direction. However, the interacting ground motions can significantly require the ductility factors in both directions. The demand becomes greater when one additional horizontal component and the vertical component are included. The ductilities of columns are generally demanded more at the third-quarter floor level (measured from the ground level) and the top floor. (IV) The elasto-plastic model is very sensitive to interacting ground motions and, thus, exhibits much larger lateral displacements and ductilities than the inelastic model. Vertical displacements are not sensitive to mathematical models.

The above observations apparently reveal that ATC-3 has not adequately specified the effect of the interacting ground motions on so-called regular buildings⁴ (symmetric), because the recommended superposition technique cannot take account of the interacting effect on moments and the vertical motion effect on axial forces. In addition, larger ductility requirements should be specified at certain floor levels.

VI. ACKNOWLEDGMENTS

This research project was sponsored by the National Science Foundation under Grant No. ENV-7518372-A01. The authors deeply appreciate the financial support and the continuous encouragement and advice that Dr. S.C. Liu, Program Manager, provided during the course of the investigation.

VII. REFERENCES

1. Cheng, F.Y. and Kitipitayangkul, P. (1979), Investigation of the Effect of 3-D Parametric Earthquake Motions on Stability of Elastic and Inelastic Building Systems, Report No. 1, available at the U.S. NTIS and the University of Missouri-Rolla.
2. Cheng, F.Y. (1979), "Inelastic Analysis of Dynamic Space Frameworks", Proc. of 7th Conf. on Electronic Computations, ASCE, pp. 537-52.
3. Bathe, K.J. and Wilson, E.L. (1976), Numerical Methods in Finite Element Analysis, Chapter 8, Prentice-Hall, New Jersey.
4. ATC-3-Tentative Provisions for the Development of Seismic Regulations for Buildings, NBS SP-510, 1978.

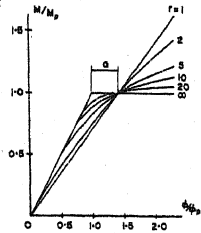


Fig. 1. Steel Models

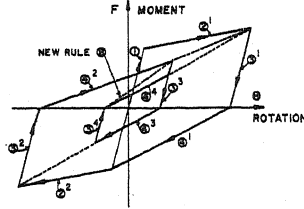
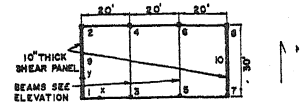


Fig. 2. Concrete Hysteresis



Floor Plan
TOTAL FLOOR MASS = $M(Kg \cdot sec^2/m)$

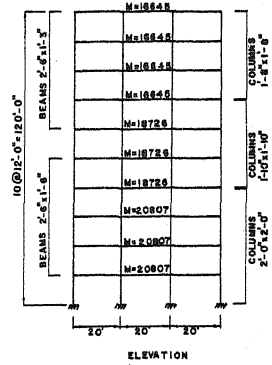


Fig. 3. Reinforced Concrete Building

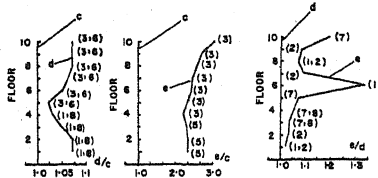
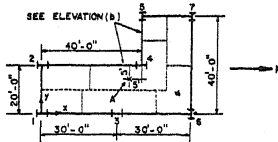
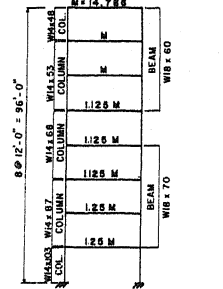


Fig. 4. Response Comparisons of Fig. 3



(a) FLOOR PLAN
TOTAL FLOOR MASS, $M(Kg \cdot sec^2/m)$
 $M = 14,788$



(b) TYPICAL ELEVATION

Fig. 5. Steel Building

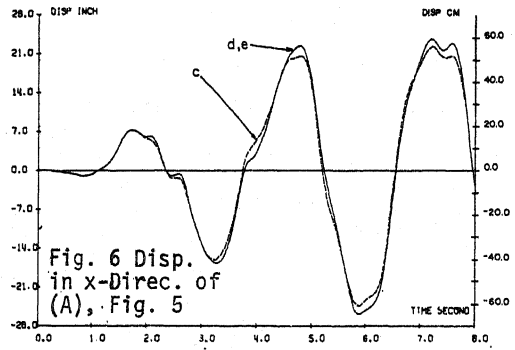


Fig. 6. Disp. in x-Direc. of (A), Fig. 5

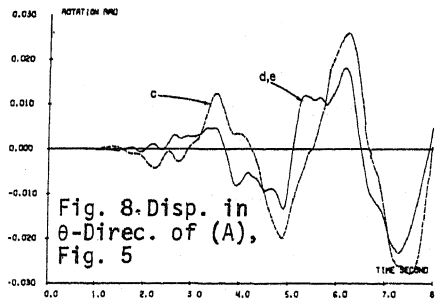


Fig. 8. Disp. in θ -Direc. of (A), Fig. 5

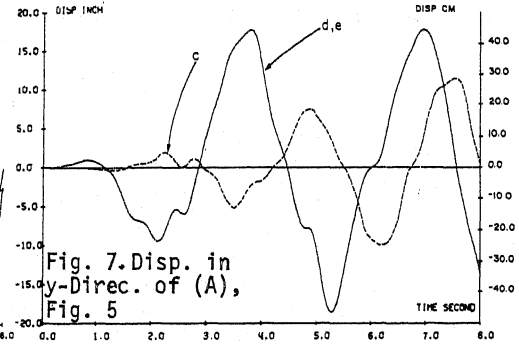
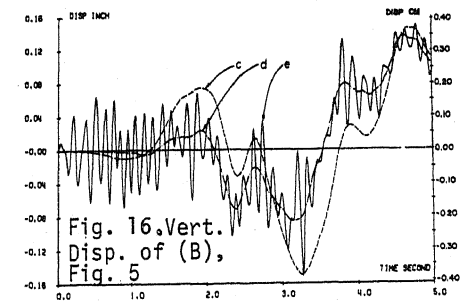
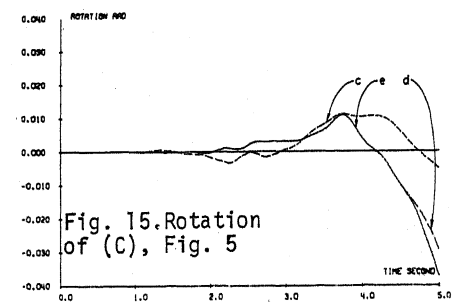
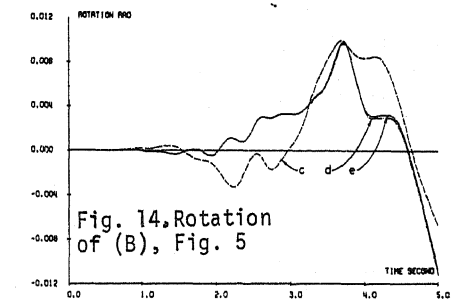
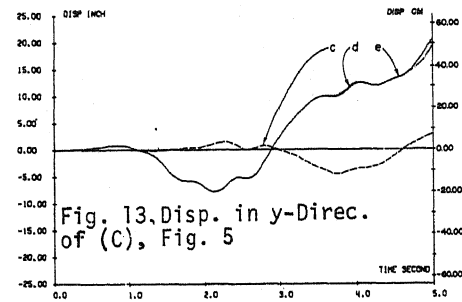
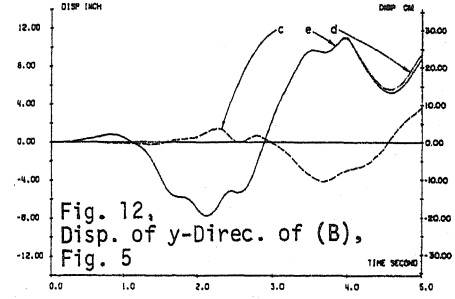
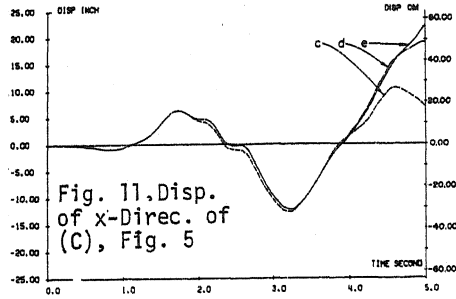
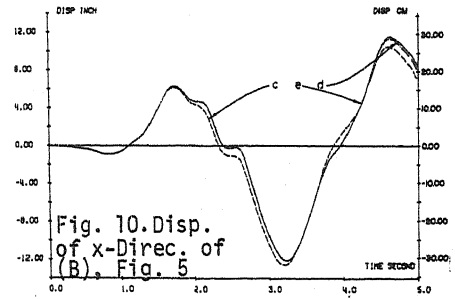
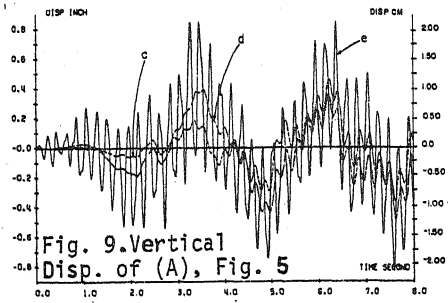


Fig. 7. Disp. in y-Direc. of (A), Fig. 5



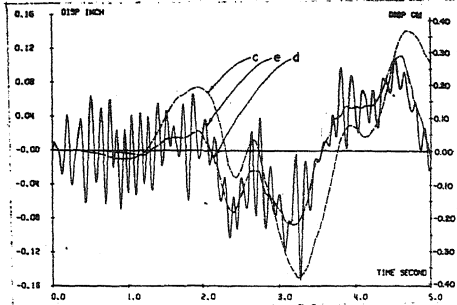


Fig. 17. Vert. Disp. of (C), Fig. 5

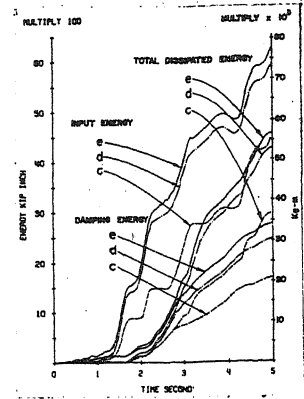


Fig. 18. Energy Comp. of (B), Fig. 5

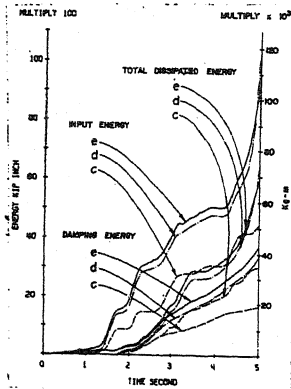


Fig. 19. Energy Comp. of (C), Fig. 5

Fig. 20. Energy Comparison of (D), Fig. 5

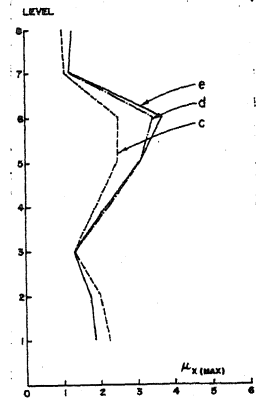
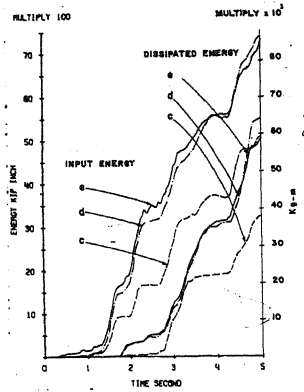


Fig. 21. Ductilities of (B), Fig. 5

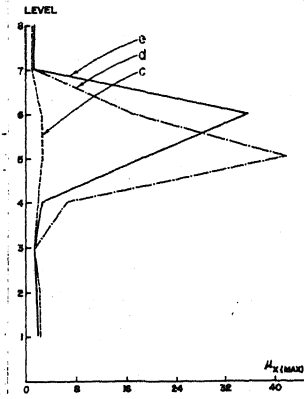


Fig. 22. Ductilities of (C), Fig. 5

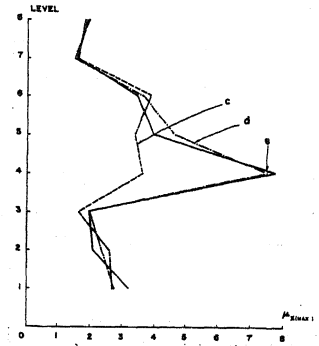


Fig. 23. Ductilities of (D), Fig. 5